

# High-intensity pulsed source of space-time and polarization double-entangled photon pairs

Yoon-Ho Kim,<sup>\*</sup> Sergei P. Kulik,<sup>†</sup> and Yanhua Shih

Department of Physics, University of Maryland, Baltimore County, Baltimore, Maryland 21250

(Received 4 April 2000; published 13 June 2000)

Two spatially separated type-I nonlinear crystals are pumped by femtosecond laser pulses to create entangled photon pairs in the process of spontaneous parametric down-conversion. The two-photon entangled state exhibits high-visibility quantum interference for both polarization and space-time variables without the need of stringent spectral postselection by using narrow-band filters. The visibility is insensitive to the thickness of the crystals, unlike in the case of pulse pumped type-II parametric down-conversion; therefore the intensity can be easily increased by using thick nonlinear crystals. This method will be indispensable in experiments that require a pulsed source of entangled photon pairs, such as generation of multiphoton entangled states, quantum teleportation, and quantum communications.

PACS number(s): 42.50.Dv, 03.65.Bz, 42.65.Ky

Femtosecond pulse pumped spontaneous parametric down-conversion (SPDC) is very useful for the realization of certain types of experiments in quantum optics, such as generation of multiphoton entangled states, quantum teleportation, quantum communications, etc [1]. Since the 1990s type-II SPDC has been used extensively as a source of two-photon entangled states for space-time, polarization, and space-time – polarization double entanglement [2]. However, type-II SPDC has its limitation for femtosecond applications. The degree of entanglement of the two-photon state generated in type-II SPDC pumped by femtosecond pulses strongly depends on the thickness of the nonlinear crystal [3–5]. To obtain high-visibility quantum interference in pulse pumped type-II SPDC, one can *only* do the following: (i) use a thin BBO crystal ( $\approx 100 \mu\text{m}$ ) or (ii) accomplish spectral postselection by using narrow-band filters [6,7]. Both methods severely limit the available entangled photon flux reaching the detectors.

In this paper, we experimentally demonstrate two methods for generating a *pulsed source of space-time and polarization double-entangled photon pairs* that exhibit high-visibility quantum interference. The visibility is shown to be insensitive to the thickness of the crystals and the bandwidth of the filters. Therefore, high-intensity pulsed entangled photon pairs can be easily generated by simply using thicker nonlinear crystals, which has a great advantage over pulse pumped type-II SPDC.

It has recently been shown by Kwiat *et al.* and by Burlakov *et al.* that SPDC created from two spatially separate type-I nonlinear crystals pumped by cw laser beams exhibit high-visibility quantum interference [8,9]. In both cases, temporal compensation was not an important issue. We shall demonstrate in this paper that pulse pumped type-I SPDC in the two-crystal scheme requires great attention to the overlapping of the two-photon amplitudes temporally, unlike cw pumped two-crystal cases.

Consider the experimental setup shown in Fig. 1. A fre-

quency doubled radiation of a mode-locked Ti:sapphire laser is used to pump two type-I BBO crystals. The pump has a pulse width of  $\approx 80$  fsec and a central wavelength of 400 nm. The repetition rate of the pump pulse is 82 MHz. The pump is polarized at  $45^\circ$ . A BBO crystal is placed in each arm of a balanced Mach-Zehnder interferometer (MZI). The thickness of both BBO crystals is 3.4 mm. The pump beam is then blocked by mirrors  $M_3$  and  $M_4$  while transmitting 800-nm collinear degenerate SPDC. The optic axes of the two BBO crystals are orthogonal to each other: the optic axis of the BBO ( $\text{BBO}_1$ ) in the arm that contains  $M_3$  is oriented in the horizontal ( $\odot$ ) plane and the other BBO ( $\text{BBO}_2$ ) is oriented vertically ( $\updownarrow$ ). Due to type-I phase matching in the BBO's, the pair of SPDC photons created from  $\text{BBO}_1$  are vertically ( $V$ ) polarized and the SPDC from  $\text{BBO}_2$  is polarized horizontally ( $H$ ). At each output port of the nonpolarizing beam splitter (NPBS), a detector package consisting of a Glan-Thompson analyzer ( $A_1, A_2$ ), an interference filter ( $F_1, F_2$ ), and a single-photon detector (EG&G SPCM-AQ-142) are placed. Interference filters are mainly used for alignment purposes and to suppress background noise from the pump.

The simplified version of the quantum state *after* NPBS can be written as (we only consider coincidence contributing terms)

$$|\psi\rangle = |V_1, V_2\rangle + \exp(i\varphi)|H_1, H_2\rangle, \quad (1)$$

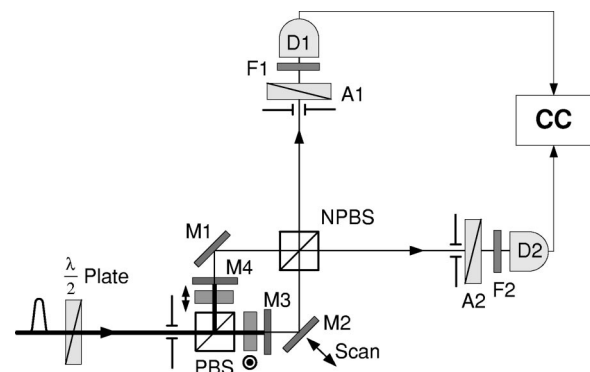


FIG. 1. Experimental setup. A type-I BBO crystal is placed in each arm of a balanced Mach-Zehnder interferometer. CC is the coincidence circuit.

<sup>\*</sup>Email address: yokim@umbc.edu

<sup>†</sup>Permanent address: Department of Physics, Moscow State University, Moscow 119899, Russia.

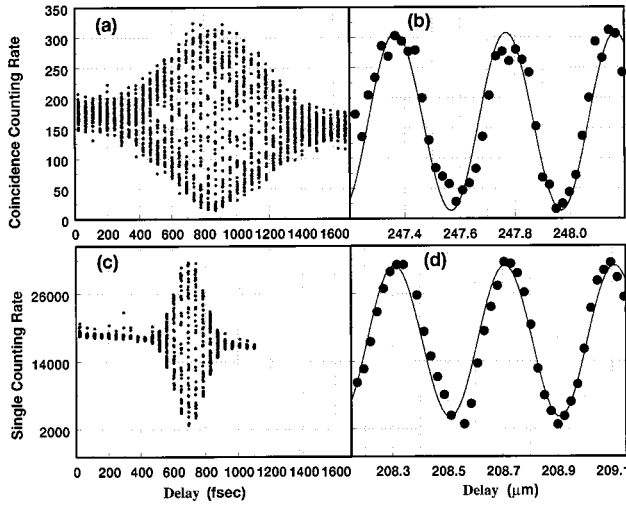


FIG. 2. Experimental data. (a) An interference pattern is observed in coincidences by scanning  $M_2$ . Each column of the data looks like (b). Note that the modulation period is 400 nm. 10-sec accumulation time and 10-nm filters are used. With 40-nm filters, the visibility is slightly reduced but the width and the shape of the interference fringe remain the same. (c) and (d) with BBO and the uv reflecting mirrors removed from the interferometer. The first-order pump pulse interference is observed in the single counting rates. A 0.5-sec accumulation time is used.

where  $\varphi$  is the relative phase between the two terms. This is a polarization entangled Bell-type state, provided that the two terms  $|V_1, V_2\rangle$  and  $|H_1, H_2\rangle$  are made indistinguishable. If the MZI is balanced, the two terms overlap in time and become indistinguishable temporally. Equation (1) shows that quantum interference will occur between the biphoton amplitudes emitted from two spatially separate crystals, and  $\varphi$  can be interpreted as the relative phase between them. It is very important to note that if the two terms in Eq. (1) are distinguishable in time, it is *not* a Bell state, although it looks like one. It can be easily demonstrated by moving the mirror  $M_2$  to an unbalanced position.

Observation of high-visibility quantum interference is a test of the degree of quantum entanglement. To demonstrate the space-time quantum interference of the entangled state in Eq. (1), we set the angles of the analyzers  $A_1$  and  $A_2$  at  $45^\circ$  and scan  $M_2$  by an encoder driver. In this measurement, the pump beam average power in each arm of the MZI is  $\approx 10$  mW. As expected, high-visibility quantum interference is observed in coincidences, see Figs. 2(a) and 2(b), while the interferometer is balanced. As  $M_2$  moves away from the balanced position, the interference visibility is reduced and reaches zero when the two wave packets in Eq. (1) are completely distinguishable. Note in Fig. 2(b) that the modulation period of the interference fringe is 400 nm, which is the pump central wavelength, although the SPDC wavelength is 800 nm. This is a well-known two-photon effect [2,8,9]. In Figs. 2(c) and 2(d), pump pulse interference is demonstrated in comparison with the SPDC interference. This is done by simply removing the BBO crystals and the uv reflecting mirrors from the MZI. Note that the observed envelope of first-order pump pulse interference is narrower than the width of

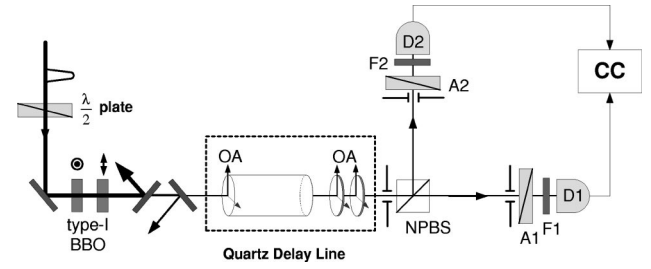


FIG. 3. Experimental setup. Quartz delay line introduces relative delays between the biphoton amplitudes created in the first and second BBO.

the SPDC two-photon interference.

This unusual effect can only be observed in the case of pulse pump with a thick crystal ( $l_{coh} < L$ , where  $l_{coh}$  is the coherence length of the pump pulse and  $L$  is the crystal thickness). Here we provide a simple physical description and a detailed theoretical treatment will be discussed elsewhere. Due to the group velocity difference between the pump pulse and the SPDC, the SPDC photon pairs travel faster in the BBO. Since the SPDC process can take place at any location with equal probability throughout the BBO, the temporal distribution of the biphoton amplitudes is calculated to be

$$\left( \frac{1}{u_p(\Omega_p)} - \frac{1}{u_o(\Omega_p/2)} \right) L \equiv D + L, \quad (2)$$

where  $u_p(\Omega_p)$  and  $u_o(\Omega_p/2)$  are the group velocities of the pump and the SPDC, respectively, and  $\Omega_p$  is the central frequency of the pump pulse spectrum [10]. (See Fig. 5 for a qualitative physical explanation.) One can then overlap the two biphoton amplitudes  $|V_1, V_2\rangle$  (created from BBO<sub>1</sub>) and  $|H_1, H_2\rangle$  (created from BBO<sub>2</sub>) by moving the mirror  $M_2$  to the balanced position. The width of the envelope of the interference fringe should be equal to the width of the convolution of the two amplitudes of the biphoton distribution. The observed data agree well with Eq. (2).

We have so far demonstrated an alternative method of generating pulsed entangled photon pairs and the importance of temporally overlapping  $|V_1, V_2\rangle$  and  $|H_1, H_2\rangle$  biphoton wave packets. This method, however, requires a highly stable MZI. One then wonders whether two crystals can be placed collinearly without the need of the MZI in the femto-second pulse case. We have also performed this experiment. See Fig. 3. Two orthogonally oriented type-I BBO crystals are placed collinearly and pumped by  $45^\circ$  polarized femto-second pulses. The SPDC is separated from the pump by using two specially coated mirrors that reflect the 400-nm pump beam while transmitting the 800-nm SPDC. The collinear degenerate SPDC then passes through the quartz delay line consisting of a set of quartz rods and two thin quartz plates (600  $\mu\text{m}$  each). The optic axes of the quartz are oriented vertically so that  $V$  polarized photons are delayed relative to  $H$  polarized photons. Therefore it basically delays the SPDC created from the first BBO relative to the SPDC from the second BBO, and the delay is proportional to the number of quartz rods used in the delay line. The use of two thin

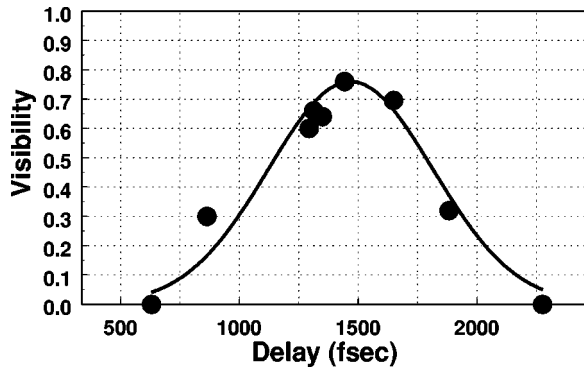


FIG. 4. Visibility versus the relative delay between  $|V_1, V_2\rangle$  and  $|H_1, H_2\rangle$  in the case of 10-nm filters. Note that maximum visibility is observed when the delay is 1.5 psec. The solid line is the Gaussian fitting and is solely used to estimate the width of the envelope. With the 40-nm filter, the maximum visibility is slightly reduced to 65%.

quartz plates is to introduce subwavelength delay by tilting them in the opposite directions. The quantum state *after* NPBS is the same as in Eq. (1). As mentioned above, the two terms  $|V_1, V_2\rangle$  and  $|H_1, H_2\rangle$  should be made indistinguishable to observe high-visibility quantum interference. In our setup, this temporal compensation is done by using the quartz delay line—it delays  $|V_1, V_2\rangle$  relative to  $|H_1, H_2\rangle$  to overlap the two terms in time.

We first observed the space-time interference in the following way. Both polarization analyzers  $A_1$  and  $A_2$  are oriented at  $45^\circ$  and the quartz delay is increased by introducing a set of quartz rods. At each “big” delay (or compensation) introduced by the quartz rods, we tilt the two thin quartz plates to introduce subwavelength phase delay  $\varphi$ . The visibility of the space-time quantum interference is measured and plotted in Fig. 4. Note that interference visibility is maximum when the introduced compensation is  $\approx 1.5$  psec. This can be explained in a simple physical picture shown in Fig. 5. At the second BBO, the SPDC from the first BBO ( $|V, V\rangle$ ) travels faster while SPDC process occurs in the second BBO by the vertical component of the pump beam that creates amplitude  $|H, H\rangle$ . After the two BBO crystals, therefore,  $|V, V\rangle$  and  $|H, H\rangle$  are separated by 1.5 psec, which is determined by the thickness of the BBO crystal. The quartz delay line overlaps these two terms so that they are indistinguishable in time.

Since the phase term  $\varphi$  in Eq. (1) can be easily varied, the polarization Bell states [11] can also be easily prepared. The

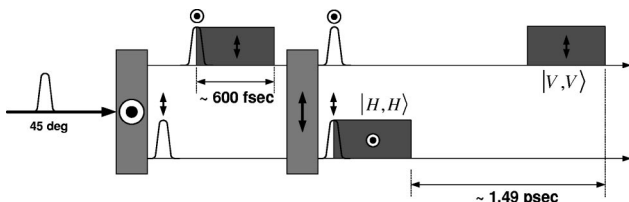


FIG. 5. Temporal distribution of the biphoton. The width (600 fsec) of the biphoton distribution is represented by the shaded rectangles. Note that the distance between the two BBO crystals is *not* an important factor in the experiment.

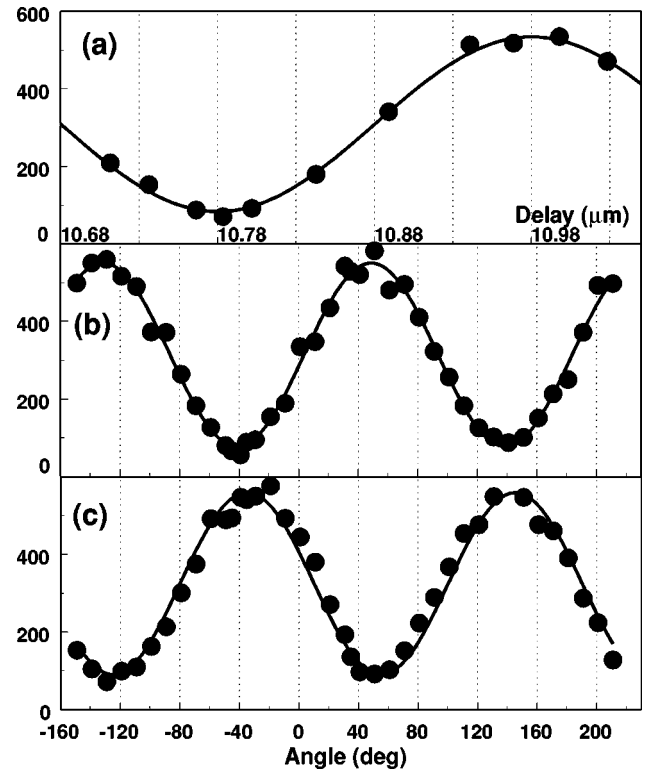


FIG. 6. (a) Space-time interference is observed by varying the phase  $\varphi$ . Note that the modulation period is 400 nm. (b) Polarization interference for the state  $|\Phi^-\rangle$  at the space-time destructive interference point. (c) Polarization interference for the state  $|\Phi^+\rangle$  at the space-time constructive interference point. The well-known  $\pi$  phase shift is demonstrated. The data accumulation time is 30 sec.

delay is set to 1.5 psec and a subwavelength phase delay  $\varphi$  is introduced by the two thin quartz plates. In Fig. 6(a), space-time interference is observed by varying  $\varphi$ . The polarization Bell states

$$|\Phi^+\rangle = |X_1, X_2\rangle + |Y_1, Y_2\rangle \quad \text{for } \varphi = 0,$$

$$|\Phi^-\rangle = |X_1, X_2\rangle - |Y_1, Y_2\rangle \quad \text{for } \varphi = \pi$$

can then be prepared. Note that  $|X\rangle$  and  $|Y\rangle$  form the orthogonal basis of an *arbitrary* right-hand coordinate system where the SPDC propagation direction is taken to be in the  $z$  direction. Experimentally,  $|\Phi^+\rangle$  and  $|\Phi^-\rangle$  can be identified by constructive and destructive quantum interference, respectively. The above polarization Bell states should exhibit polarization interference in coincidence counting rates between the two detectors while the single counting rates remain constant, i.e.,

$$R_c \propto |\langle \theta_2, \theta_1 | \Phi^\pm \rangle|^2 \propto \cos^2(\theta_1 \mp \theta_2). \quad (3)$$

Note that  $\theta_1$  and  $\theta_2$  are *arbitrary* angles. The data presented in Fig. 6(b) are for  $|\Phi^-\rangle$  and in Fig. 6(c) are for  $|\Phi^+\rangle$ . For both Figs. 6(b) and 6(c), the angle of  $A_1$  ( $\theta_1$ ) is fixed at  $45^\circ$  and  $A_2$  is rotated. To make sure the state is really a polarization Bell state, we have repeated the measurement for many

different angles of  $A_1$ . The observed visibility has remained the same, which means that the state we observed is truly a polarization Bell state.

The other two polarization Bell states ( $|\Psi^+\rangle$  and  $|\Psi^-\rangle$ ) can also be prepared by inserting a  $\lambda/2$  plate in one of the two output ports of the NPBS. Note that the observed visibility in this experiment is much higher than any pulse pumped type-II SPDC experiments using such a thick crystal even with reasonably narrow-band filters. The collinear method requires much less work and has proved to be very stable. However, it might be difficult to apply in nondegenerate SPDC applications, since complicated compensation has to be introduced [12].

In summary, we have demonstrated two different methods, which are based on the same physical principle, to generate a pulsed source of polarization and space-time double-entangled photon pairs by using two separate type-I crystals pumped by femtosecond laser pulses. Unlike pulse pumped

type-II SPDC, high-visibility quantum interference is observed without stringent spectral postselection, and the visibility is insensitive to the crystal thickness and the filter bandwidth. Note also that nonmaximally entangled states can easily be generated by simply rotating the  $\lambda/2$  plate placed in the pump beam. We believe that these alternative methods will be indispensable in experiments that require a pulsed source of entangled-photon pairs.

*Note added in proof.* After this paper was accepted for publication, we achieved  $>90\%$  visibility with 40-nm filters in the collinear setup shown in Fig. 3.

We would like to thank M.H. Rubin for helpful discussions. This research was supported, in part, by the Office of Naval Research and the National Security Agency. S.P.K. also thanks the Russian Fund for Fundamental Research, Grant No. 99-02-16419, for partially supporting his visit to UMBC.

- 
- [1] D.M. Greenberger *et al.*, Am. J. Phys. **58**, 1131 (1990); C.H. Bennett *et al.*, Phys. Rev. Lett. **70**, 1895 (1993); D. Bouwmeester *et al.*, Nature (London) **390**, 575 (1997); D. Boschi *et al.*, Phys. Rev. Lett. **80**, 1121 (1998); D. Bouwmeester *et al.*, *ibid.* **82**, 1345 (1999).
- [2] T.E. Kiess *et al.*, Phys. Rev. Lett. **71**, 3893 (1993); Y.H. Shih *et al.*, Phys. Rev. A **50**, 23 (1994); T.B. Pittman *et al.*, *ibid.* **52**, R3429 (1995); P.G. Kwiat *et al.*, Phys. Rev. Lett. **75**, 4337 (1995); D.V. Strekalov *et al.*, Phys. Rev. A **54**, R1 (1996); T.B. Pittman *et al.*, Phys. Rev. Lett. **77**, 1917 (1996); K. Mattle *et al.*, *ibid.* **76**, 4656 (1996).
- [3] T.E. Keller and M.H. Rubin, Phys. Rev. A **56**, 1534 (1997).
- [4] W.P. Grice and I.A. Walmsley, Phys. Rev. A **56**, 1627 (1997); J. Peřina, Jr. *et al.*, *ibid.* **59**, 2359 (1999).
- [5] G. Di Giuseppe *et al.*, Phys. Rev. A **56**, R21 (1997); W.P. Grice *et al.*, *ibid.* **57**, R2289 (1998); M. Atatüre *et al.*, Phys. Rev. Lett. **83**, 1323 (1999).
- [6] M. Atatüre *et al.*, Phys. Rev. Lett. **84**, 618 (2000).
- [7] Y.-H. Kim, S.P. Kulik, M.H. Rubin, and Y.H. Shih (unpublished). To claim polarization entangled states, for example,  $|\Phi^\pm\rangle = |V_1, V_2\rangle \pm |H_1, H_2\rangle$ , one needs to observe quantum interference,  $R_c \propto \cos^2(\theta_1 \mp \theta_2)$ , for all possible angles ( $\theta_1$  and  $\theta_2$ ) of the analyzers ( $A_1$  and  $A_2$ ). In Ref. [6], the authors only measured the correlation between  $H$  and  $V$  photons. For angles other than  $H$  and  $V$ , the visibility is lowered and disappears.
- [8] P.G. Kwiat *et al.*, Phys. Rev. A **60**, R773 (1999); A.G. White *et al.*, Phys. Rev. Lett. **83**, 3103 (1999).
- [9] A.V. Burlakov *et al.*, Phys. Rev. A **60**, R4209 (1999); A.V. Burlakov and D.N. Klyshko, Pis'ma Zh. Éksp. Teor. Fiz. **69**, 795 (1999) [JETP Lett. **69**, 839 (1999)].
- [10] Note that the biphoton width is determined by  $D''L$  in type-I SPDC, where  $D'' = d^2K/d\Omega^2|_{\Omega=\Omega_p/2}$  [3]. This value depends on the spectral bandwidth of the filters placed in front of the detectors. Since  $D''L \ll D_+L$ , in our experiment, the observed width of the envelope of the interference fringe does not depend on the filter bandwidth.
- [11] S.L. Braunstein, A. Mann, and M. Revzen, Phys. Rev. Lett. **68**, 3259 (1992).
- [12] Y.-H. Kim, S.P. Kulik, and Y.H. Shih (unpublished). In this work, both MZI and collinear methods are applied to nondegenerate SPDC applications. Under appropriate conditions, high-visibility ( $>90\%$ ) quantum interference was observed.